Scientific Reports

https://doi.org/10.1038/s41598-026-53436-0

Article in Press

Research on improved nonlinear viscoelastic-plastic damage model of rock and parameter identification

Received: 16 March 2026

Accepted: 12 May 2026

Published online: 19 May 2026

Cite this article as: Tian X., Jia B., Sun D. *et al.* Research on improved nonlinear viscoelastic-plastic damage model of rock and parameter identification. *Sci Rep* (2026). https://doi.org/10.1038/s41598-026-53436-0

Xingchao Tian, Benchao Jia, Dingyu Sun, Zhen Cheng, Tiejun Tao & Mengqiang Pan

Research on improved nonlinear viscoelastic-plastic damage model of rock and parameter identification

Xingchao TIAN[1], Benchao JIA[2], Dingyu SUN[2], Zhen CHENG[2],Tiejun TAO[3,]*

Mengqiang PAN[1]

1. College of Civil Engineering, Transportation and Water Conservancy, Guizhou Institute of Technology, Guiyang 550025, China.

2. Guizhou Chengqian Minerals Co., Ltd., Zunyi 563131, China.

3. College of Mining, Guizhou University, Guiyang 550025, China

Correspondence should be addressed to Tiejun TAO; tjtao@gzu.edu.cn

Abstract: How to accurately characterize the nonlinear characteristics of rock mass creep has long been a research hotspot. The traditional Kelvin model cannot accurately characterize the nonlinear variation process in the decay creep stage and the dual characteristics of power function and exponential function in the accelerated creep stage, so it needs to be modified. Based on nonlinear rheological theory and damage theory, this paper establishes a damage creep model that simultaneously considers instantaneous elastic strain, nonlinear viscoelastic strain, viscous strain, and nonlinear viscoplastic strain. The differential damage constitutive equations under one-dimensional and three-dimensional stress states are derived, the method for determining model parameters is presented, and the model is verified based on the triaxial compression creep test results of sandstone. Meanwhile, a sensitivity analysis is performed on the parameters of the modified model. The results show that the modified model can accurately reflect the entire creep process of sandstone under different confining pressures. In uniaxial compression creep tests, the peak strain is most sensitive to changes in the parameters η_2 and η_4. Under high confining pressure, the peak strain is most sensitive to changes in the parameters β, n, and η_4.

Keywords: Nonlinearity, Viscoelastoplasticity, Damage model, Parameter identification, Sensitivity analysis

Nomenclature table

Symbol	Physical meaning	Symbol	Physical meaning
E_1	The elastic modulus of the elastic body	δ_{ij}	Kronecker tensor
E_2	The elastic modulus of the nonlinear Kelvin body	t_f	Time to creep failure
η_1	Viscosity coefficient of the nonlinear Kelvin body	ε_{ij}	Total strain under three-dimensional stress state
η_3	Viscosity coefficient of the viscous body	ε_{ij}^{e}	Strain at each stage under three-dimensional stress state
E_3	Elastic modulus of the nonlinear damage viscoplastic body	ε_{ij}^{ve}	
η_3	Viscosity coefficient of the nonlinear damage viscoplastic body	ε_{ij}^{v}	
η_4	Viscosity coefficient of the nonlinear damage viscoplastic body	ε_{ij}^{vp}	
D	Damage variable	G_1, K_1	Shear modulus and bulk modulus of the elastic body
σ_s	Yield strength of rock	G_2	Shear modulus of the nonlinear Kelvin body
σ_e, ε_e	Stress and strain in the elastic deformation stage	F	Rock yield function
σ_{ve}, ε_{ve}	Stress and strain in the decay creep stage	F_0	Initial value of rock yield function
σ_v, ε_v	Stress and strain in the steady creep stage	K	Specified constants
σ_{vp}, ε_{vp}	Stress and strain in the accelerated creep stage	Q	Plastic potential function
σ, ε	Total stress and total strain	J_2	Second invariant of the stress deviator
β	Time-dependent constant in the nonlinear Kelvin body	I_1	First invariant of the stress tensor
C	Material parameters related to damage variable D	α, k	Material parameters
n		φ, c	The internal friction angle and cohesion of rock
σ_{ij}, ε_{ij}	Stress tensor and strain tensor	$RMSE$	Root Mean Square Error
S_{ij}, e_{ij}	Deviatoric stress tensor and deviatoric strain tensor	R^2	Coefficient of determination
σ_m, ε_m	Spherical stress and spherical strain	$\delta\varepsilon$	Strain rate

1 Introduction

The creep characteristics of rock masses are directly related to the safety and long-term stability of engineering construction. How to accurately characterize the nonlinear creep characteristics of rock masses is a hot and difficult issue in current research. Zhou et al. [1] summarized important research directions regarding the creep damage mechanism of rocks. Tarifard et al. [2] discussed the main characteristics of current rock creep models and evaluated the effectiveness of these models in simulating the accelerated creep stage. Yang et al. [3-4] proposed a nonlinear creep model considering the coupling effect of long-term creep and short-term disturbance, and verified the model through experiments. Fang et al. [5-7] investigated the compressive mechanical properties of rocks using numerical methods and established the corresponding constitutive equations. Liu et al. [8] investigated the interaction characteristics between fault creep and rock creep. Yang et al. [9] investigated the mechanical response of salt rock to creep under different stress conditions and proposed a damage model to characterize the full-stage creep behavior of salt rock. Chen et al. [10] studied the creep fracture characteristics of sandstone and established the relationship between micro-damage, macro-damage, and fracture. Liu et al. [11] adopted the two-phase field method to simulate the creep characteristics of rocks and carried out experimental verification.

In traditional creep models, all parameters are constant. Therefore, no matter how complex the element structure is, it is impossible to accurately characterize the creep characteristics of rock masses. Especially when the stress level of a rock mass exceeds its long-term bearing capacity, nonlinear creep effects will occur [12-13]. In recent years, scholars worldwide have proposed two main solutions to address such problems. One is to establish variable-parameter creep models by considering the time dependence of model parameters, or construct nonlinear creep models by connecting nonlinear elements in series [14-16]. The other is to introduce damage variables into the creep constitutive equation according to Lemaitre's strain equivalence principle, so as to establish a damage creep model [17-19].

At present, fruitful achievements have been made in the research on rock creep models, but some problems still remain. (1) Unscientific parameter identification methods. Existing studies often adopt regression analysis or the least square method to process triaxial creep experimental data by fitting one-dimensional creep equations. However, one-dimensional creep equations do not contain confining pressure terms, so their direct use in determining the parameters of three-dimensional models lacks rationality. (2) The construction of damage creep models is not rigorous. When the damage variable is a function of time or strain, most studies derive creep equations under the assumption that model parameters are constant. Then the stress is simply replaced by effective stress to introduce the damage variable, which makes the method lack rigor. (3) Improper selection of yield criteria. In creep models containing plastic elements, the yield state of a point under three-dimensional stress conditions involves not only the selection of yield criteria, but also the determination of the plastic potential function and flow rule. However, existing studies often directly replace the three-dimensional stress state with a one-dimensional stress state. Such a direct substitution method lacks a necessary theoretical basis, and its rationality is questionable.

To avoid the above problems, an improved nonlinear viscoelastic-plastic damage model for rocks is proposed in this paper. First, the prediction models for the decay creep and accelerated creep stages are improved. The differential-type damage constitutive equations and creep equations under one-dimensional and three-dimensional stress states are derived. Then, the parameter determination method for the improved model is presented, and the model is verified based on creep test results of sandstone. Finally, a sensitivity analysis is performed on the parameters of the improved model. The research results can provide a reference for the accurate prediction of rock creep behavior under complex conditions.

2 Establishment of a nonlinear viscoelastoplastic damage model

2.1 Model Establishment

Uniaxial and triaxial compression creep tests have been carried out on different rocks in the literature, and the creep test curves are shown in Figure 1(a) [20-24]. The creep test curves can be divided into four stages: Stage □ (OA section) is the elastic deformation stage, when the stress level applied at the beginning of the creep test is lower than the yield strength of the rock, the rock produces recoverable transient elastic deformation. Stage □ (AB section) is the attenuation of the creep stage, the strain rate decreases with time. Stage □ (BC section) is the isotropic creep stage, the strain rate does not vary with time. Stage □ (CD section) for the accelerated creep stage, rock damage before the strain rate increases rapidly with time.

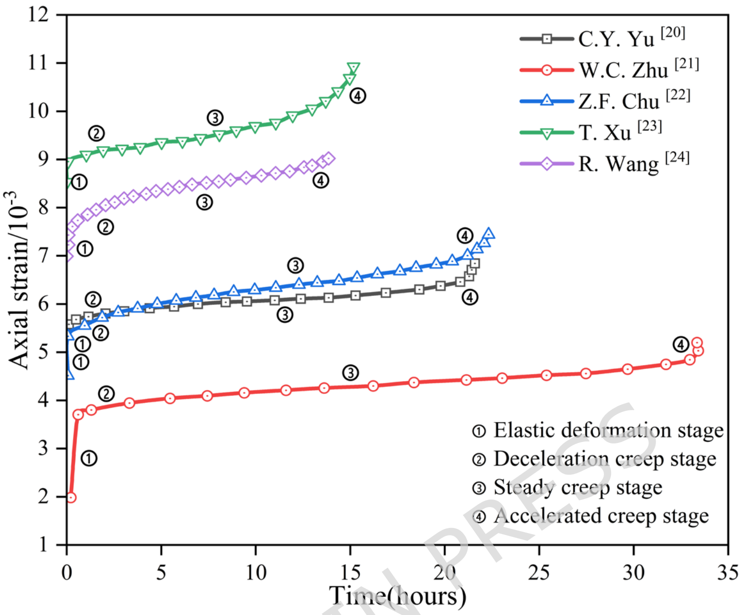

(a) Creep test curves for different types of rocks [20-24]

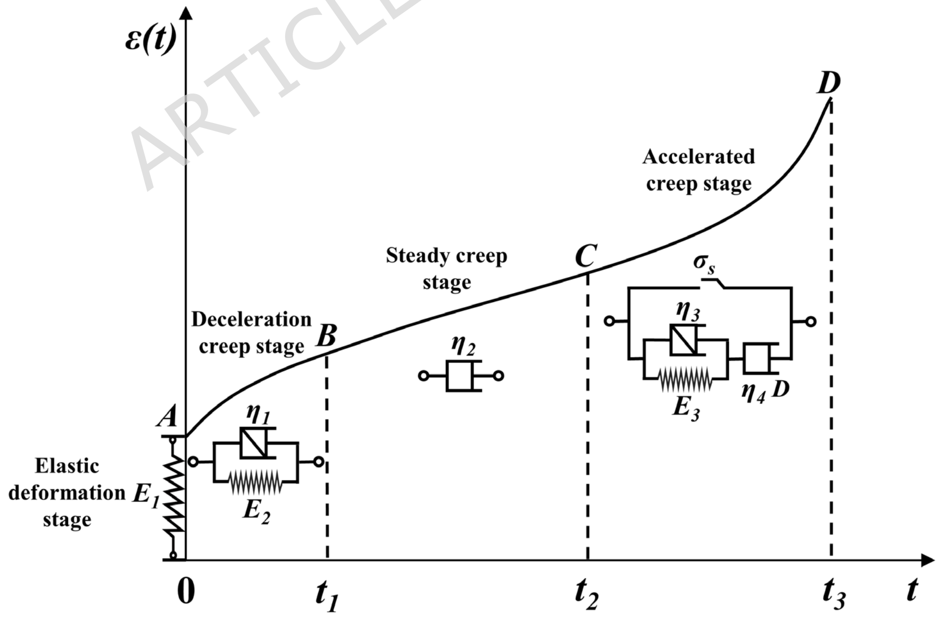

(b) Stages of the rock creep curve

Fig. 1 Rock creep curve

It can be seen from Figure 1 that the strain rate gradually decreases with time during the attenuated creep stage, exhibiting a nonlinear variation. As rocks approach failure, internal microcracks rapidly initiate, propagate and coalesce, forming macroscopic fractures. Therefore, the accelerated creep stage exhibits dual characteristics of both power function and exponential function. The traditional rock creep model is composed of an elastic element, a Kelvin element, a viscous element, and a damaged viscoplastic element in series, as shown in Figure 2(a). Among them, the dashpot of the traditional Kelvin body adopts a Newtonian fluid element, and the model parameters are constant. It exhibits poor prediction performance for the nonlinear characteristics in the attenuated creep stage. Meanwhile, the existing damaged viscoplastic element cannot accurately characterize the power-law variation characteristics of the accelerated creep stage. Therefore, it is necessary to modify the traditional rock creep model to enable it to better predict the characteristics of the attenuated creep and accelerated creep stages. In this study, a new nonlinear viscoelastic-plastic damage model is proposed by improving the traditional Kelvin body and the damaged viscoplastic element. The improved model consists of an elastic element, a nonlinear Kelvin element, a viscous element, and a nonlinear damage viscoplastic element in series, as shown in Figure 2(b). In the model schematic diagram, the spring represents the instantaneous and recoverable elastic response. The dashpot represents time-dependent and irrecoverable viscous flow. The slider represents the critical condition for triggering accelerated failure.

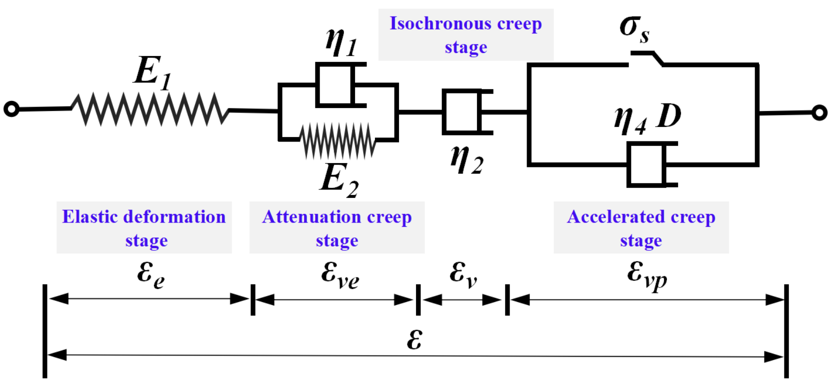

(a) Traditional creep model

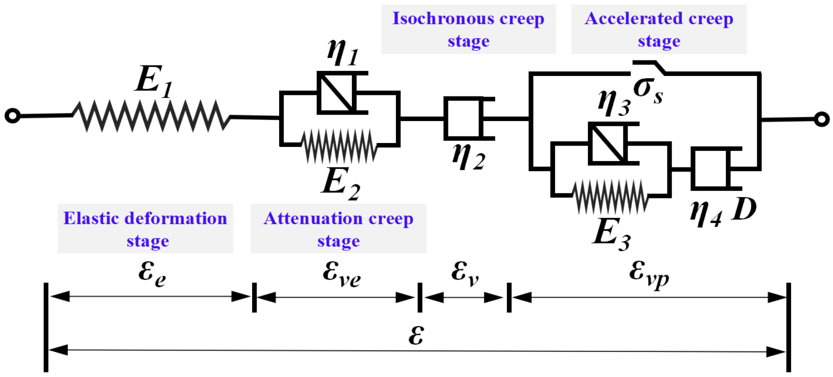

(b) Nonlinear viscoelastic-plastic damage model

Fig. 2 Rock creep model

In the elastic element, E_1 denotes the elastic modulus. In the nonlinear Kelvin element, E_2 and η_1 represent the elastic modulus and viscosity coefficient, respectively. In the viscous element, η_3 denotes the viscosity coefficient. In the nonlinear damage viscoplastic element, E_3 is the elastic modulus, η_3 and η_4 are the viscosity coefficients, D is the damage variable, and σ_s is the yield strength of the rock. ε_e, ε_{ve}, ε_v, ε_{vp} represent the strains in the elastic deformation stage, attenuated creep stage, steady-state creep stage, and accelerated creep stage, respectively. ε represents the total strain.

The modification process of the traditional Kelvin element and the damaged viscoplastic element will be described in detail in the following sections.

The traditional Kelvin element consists of a spring and a dashpot in parallel, and its constitutive equation is:

$$\sigma = \sigma_1 + \sigma_2 = E_2 \varepsilon_{ve} + \eta_1 \dot{\varepsilon}_{ve} \tag{1}$$

η_1 is the viscosity coefficient of the Newtonian dashpot and is a constant, so it cannot accurately characterize the nonlinear characteristics of the attenuated creep stage. In the current research results, the methods for modeling nonlinear creep of rocks are divided into two types [25-28]. One is to establish the nonlinear relationship between creep parameters and time. The second is to propose a new creep model and form a new nonlinear creep model in series with the traditional creep model. In this study, the former method is adopted to modify the Kelvin element, replacing the Newtonian dashpot with a non-Newtonian dashpot. Considering the time dependence of the viscosity coefficient, it is assumed that η_1 follows a power-law relationship with time during creep ($\eta_1 \cdot t^{1-\beta}$). The constitutive equation of the improved nonlinear Kelvin element is:

$$\sigma = E_2 \varepsilon_{ve} + \eta_1 t^{1-\beta} \dot{\varepsilon}_{ve} \tag{2}$$

where σ is the stress and β is a constant.

When analyzing creep problems, Equation (2) can be rewritten as a first-order linear ordinary differential equation. The creep equation of the nonlinear Kelvin model can be obtained by solving it as follows:

$$\varepsilon_{ve} = \frac{\sigma}{E_2}\left[1 - \exp(-\frac{E_2}{\eta_1 \beta} t^{\beta})\right] \tag{3}$$

After the attenuated creep stage, the rock enters the steady-state creep stage when the stress level approaches its long-term strength. At this point, a viscous element is adopted to describe its creep behavior. When the stress level exceeds the long-term strength of the rock, the rock enters the accelerated creep stage. The microcracks inside the rock rapidly propagate and coalesce, and the damage variable D gradually increases to 1, eventually leading to creep failure.

After the attenuated creep stage, when the applied stress level approaches the long-term strength of the rock, the rock will enter the steady-state creep stage. In this stage, the creep behavior of the rock can be described by a viscous element. Once the stress level exceeds the long-term strength of the rock, the rock enters the accelerated creep stage. At this time, the microcracks inside the rock rapidly propagate and coalesce with each other, and the damage variable D gradually increases until it reaches 1, eventually leading to creep failure of the rock.

Based on Lemaitre's strain equivalence principle, the constitutive equation of the damaged viscoplastic body with the introduction of the damage variable is obtained [29]:

$$\dot{\varepsilon}_{vp} = \frac{\sigma}{\eta_4 (1-D)} \tag{4}$$

In damage mechanics, the evolution equation of the damage variable D is given by [30]:

$$\dot{D}=\frac{dD}{dt}=C\cdot(\frac{\sigma}{1-D})^{n} \tag{5}$$

where C and n are material parameters.

After rearranging Equation (5) by transposing terms, integrate both sides of the equation simultaneously. Assume that D=0 at t=0, and the damage variable is D at time t. The intermediate expression for damage evolution can be obtained through calculation.

$$\frac{1-(1-D)^{n+1}}{n+1}=C\sigma^{n}t \tag{6}$$

Let the creep failure time be $t=t_f$, at which D=1. The expression for the creep failure time t_f can be obtained through solution.

$$t_{f}=\frac{1}{C(1+n)\sigma^{n}} \tag{7}$$

where t_f is the creep failure time of the rock.

Substituting $\frac{1}{(n+1)t_{f}}=C\sigma^{n}$ into Equation (6), the equation for the variation of the damage variable D with time is obtained.

$$D=1-(1-\frac{t}{t_{f}})^{\frac{1}{1+n}} \tag{8}$$

Substituting Equation (8) into Equation (4) and integrating, the creep equation of the damaged viscoplastic model under one-dimensional stress state can be obtained [31]:

$$\varepsilon_{vp}=\frac{(\sigma-\sigma_{s})t_{f}(1+n)}{\eta_{4}n}\left[1-(1-D)^{n}\right] \tag{9}$$

Although the above damaged viscoplastic model can characterize the damage behavior in the accelerated creep stage, it can only represent the exponential function characteristics. However, the accelerated creep stage exhibits both power-law and exponential characteristics. Therefore, this study further improves the damaged viscoplastic model of Equation (9). The specific improvement method is as follows: a nonlinear Kelvin body is connected in series with the viscous body, and then combined in parallel with the plastic body. This method is equivalent to adding a creep rate regulator. The creep equation of the improved nonlinear damage viscoplastic model is as follows:

$$\begin{aligned}\varepsilon_{vp} &= \frac{t_f(1+n)(\sigma-\sigma_s)}{\eta_4 n}\left[1-(1-D)^n\right]+\frac{(\sigma-\sigma_s)}{E_3}\left[1-\exp\left(-\frac{E_3}{\eta_3\beta}t^\beta\right)\right] \\ &=(\sigma-\sigma_s)\left\{\frac{t_f(1+n)}{\eta_4 n}\left[1-(1-D)^n\right]+\frac{1}{E_3}\left[1-\exp\left(-\frac{E_3}{\eta_3\beta}t^\beta\right)\right]\right\}\end{aligned} \tag{10}$$

No modifications are made to the elastic body and viscous body in this study, and their creep equations are as follows:

$$\varepsilon_e = \frac{\sigma}{E_1} \tag{11}$$

$$\varepsilon_v = \frac{\sigma}{\eta_2}t \tag{12}$$

The improved model can well characterize the nonlinear viscoelastic-plastic behavior of rock creep. Nonlinear viscoelastic deformation is time-dependent and recoverable, dominating the decelerating creep stage. The microscopic mechanism involves grain boundary sliding and time-delayed recovery of micro-pores. Nonlinear viscoplastic deformation is irrecoverable permanent deformation. It develops significantly only when the stress level exceeds the long-term strength σ_s of the rock, and dominates the accelerated creep stage. The microscopic mechanism involves the irreversible propagation of microcracks and the permanent sliding of particles. In this study, the nonlinear viscoelasticity is characterized by the improved nonlinear Kelvin body (E_2, η_1). This model accurately reflects the nonlinear time-dependent characteristics of microcrack closure and intergranular viscous deformation in rocks under stress. After stress unloading, the viscoelastic strain ε_{ve} gradually decays over time. Nonlinear viscoplasticity is characterized by the improved nonlinear damage viscoplastic body (E_3, η_3, η_4, D). When the stress exceeds the viscoplastic yield threshold, the damage variable D increases continuously with time. This leads to a continuous increase in the viscoplastic deformation rate, and the viscoplastic strain ε_{vp} exhibits no recovery after unloading.

2.2 Constitutive equation and one-dimensional creep equation

The series-parallel stress-strain relationship is obtained from the nonlinear viscoelastic-plastic damage model:

$$\begin{cases}\sigma = \sigma_{\mathrm{e}} = \sigma_{v\mathrm{e}} = \sigma_{\mathrm{v}} = \sigma_{\mathrm{v}p} \\ \varepsilon = \varepsilon_{\mathrm{e}} + \varepsilon_{v\mathrm{e}} + \varepsilon_{\mathrm{v}} + \varepsilon_{\mathrm{v}p}\end{cases} \tag{13}$$

$$\begin{cases}\sigma_e = E_1 \varepsilon_e \\ \sigma_{ve} = E_2 \varepsilon_{ve} + \eta_1 t^{1-\beta} \dot{\varepsilon}_{ve} \\ \sigma_v = \eta_2 \dot{\varepsilon}_v \\ \sigma_{vp} = E_3 \varepsilon_{\mathrm{vp}} + \eta_3 t^{1-\beta} \dot{\varepsilon}_{vp} + \sigma_s\end{cases} \tag{14}$$

where σ, ε are the stress and strain of the nonlinear viscoelastic-plastic damage model. σ_e, σ_{ve}, σ_v, σ_{vp} are the stresses in the elastic deformation stage, attenuation creep stage, isochronous creep stage, and accelerated creep stage, respectively.

According to Equation (13) and Equation (14), the intrinsic equation of the nonlinear viscoelastic-plastic damage model of rock can be calculated.

(1)When $\dot{\varepsilon}(t \to \infty) = 0, \sigma < \sigma_s$:

$$\frac{E_1 + E_2}{\eta_1 t^{1-\beta}} \sigma + \frac{\dot{\sigma}}{E_1} = \frac{E_2}{\eta_1 t^{1-\beta}} \varepsilon + \dot{\varepsilon} \tag{15}$$

(2)When $\dot{\varepsilon}(t \to \infty) > 0, \sigma < \sigma_s$:

$$\eta_2 \dot{\varepsilon} + \frac{\eta_1 \eta_2}{E_2} \ddot{\varepsilon} = \sigma + \frac{\eta_2 E_1 + \eta_2 E_2 + E_1 \eta_2 t^{1-\beta}}{E_1 E_2} \dot{\sigma} + \frac{\eta_1 \eta_2 t^{1-\beta}}{E_1 E_2} \ddot{\sigma} \tag{16}$$

(3)When $\sigma > \sigma_s$:

$$\begin{aligned}\eta_2 E_1 E_2 \dot{\varepsilon} + E_1 \eta_1 \eta_2 \ddot{\varepsilon} &= E_1 E_2 \sigma + (\eta_2 E_1 + \eta_2 E_2 + \eta_1 E_1 t^{1-\beta}) \dot{\sigma} + \eta_1 \eta_2 t^{1-\beta} \ddot{\sigma} \\ &+ A \eta_2 E_1 E_2 \dot{\sigma}' + A E_1 \eta_1 \eta_2 \ddot{\sigma}'\end{aligned} \tag{17}$$

Among them,

$$\begin{cases} \sigma' = \sigma - \sigma_s \\ A = \dfrac{t_f(1+n)}{\eta_4 n}\left[1-(1-D)^n\right] + \dfrac{1}{E_3}\left[1-\exp(-\dfrac{E_3}{\eta_3 \beta}t^{\beta})\right] \end{cases} \tag{18}$$

Similarly, the creep equation for the one-dimensional nonlinear viscoelastic-plastic damage model of rock can be calculated according to Equation (13) and Equation (14).

(1)When $\dot{\varepsilon}(t \to \infty) = 0, \sigma < \sigma_s$:

$$\varepsilon = \frac{\sigma}{E_1} + \frac{\sigma}{E_2}\left[1-\exp(-\frac{E_2}{\eta_1 \beta}t^{\beta})\right] \tag{19}$$

(2)When $\dot{\varepsilon}(t \to \infty) > 0, \sigma < \sigma_s$:

$$\varepsilon = \frac{\sigma}{E_1} + \frac{\sigma}{E_2}\left[1-\exp(-\frac{E_2}{\eta_1 \beta}t^{\beta})\right] + \frac{\sigma}{\eta_2}t \tag{20}$$

(3)When $\sigma > \sigma_s$:

$$\begin{aligned} \varepsilon = & \frac{\sigma}{E_1} + \frac{\sigma}{E_2}\left[1-\exp(-\frac{E_2}{\eta_1 \beta}t^{\beta})\right] + \frac{\sigma}{\eta_2}t \\ & (\sigma - \sigma_s)\left\{\frac{t_f(1+n)}{\eta_4 n}\left[1-(1-D)^n\right] + \frac{1}{E_3}\left[1-\exp(-\frac{E_3}{\eta_3 \beta}t^{\beta})\right]\right\} \end{aligned} \tag{21}$$

2.3 Three-dimensional creep equation

In underground space projects such as tunnels, rocks are often subjected to complex three-dimensional stresses rather than being in a one-dimensional stress state. At the same time, the aforementioned yield strength σ_s of rock is generally triaxial strength, and the current rock creep tests are mostly triaxial creep tests. Therefore, it is of great significance to derive the three-dimensional creep equation of rocks.

The following two assumptions are made when deriving the three-dimensional creep equation for rocks: (1) rock damage is produced only in the accelerated creep stage; (2) the damage in all directions of the rock remains consistent.

The total strain of the nonlinear viscoelastic-plastic damage model under three-dimensional stress state can be expressed as:

$$\varepsilon_{ij} = \varepsilon_{ij}^{e} + \varepsilon_{ij}^{ve} + \varepsilon_{ij}^{v} + \varepsilon_{ij}^{vp} \tag{22}$$

where ε_{ij} represents the total strain under three-dimensional stress state. $\varepsilon_{ij}^{e}, \varepsilon_{ij}^{ve}, \varepsilon_{ij}^{v}, \varepsilon_{ij}^{vp}$ represent the strain at each stage under three-dimensional stress state, respectively.

Under three-dimensional stress state, the stress and strain at any point inside the elastic rock can be decomposed into spherical tensor and deviatoric tensor [32].

$$\begin{cases} \sigma_{ij} = S_{ij} + \delta_{ij}\sigma_m \\ \varepsilon_{ij} = e_{ij} + \delta_{ij}\varepsilon_m \end{cases} \tag{23}$$

where σ_{ij} and ε_{ij} are the stress tensor and strain tensor, respectively. S_{ij} and e_{ij} are the deviatoric stress tensor and deviatoric strain tensor, respectively. σ_m and ε_m are the mean spherical stress and mean spherical strain, respectively. δ_{ij} is the Kronecker delta tensor.

According to the generalized Hooke's law:

$$\begin{cases} e_{ij} = \dfrac{1}{2G_1} S_{ij} \\ \varepsilon_m = \dfrac{1}{3K_1} \sigma_m \end{cases} \tag{24}$$

Where G_1 and K_1 are the shear modulus and bulk modulus of the elastic body, respectively.

Substituting Equation (22) into Equation (21) and rearranging yields the three-dimensional creep equation of the elastic body:

$$\varepsilon_{ij}^{e} = \frac{1}{2G_1} S_{ij} + \frac{1}{3K_1} \delta_{ij}\sigma_m \tag{25}$$

Under three-dimensional stress state, the viscoelastic deformation of rock is mainly manifested as shear deformation (the deviatoric tensor part). Volumetric deformation is regarded as elastic, so viscoelastic analysis is only performed on deviatoric stress and deviatoric strain. In the generalized Hooke's law, the constitutive relation between deviatoric stress and deviatoric strain is:

$$S_{ij} = 2G_2 e_{ij} \tag{26}$$

where G_2 is the shear modulus of the nonlinear Kelvin body, with $G_2=E_2/2(1+\mu)$.

Substituting Equation (24) into Equation (3) and rearranging yields the three-dimensional creep equation of the nonlinear Kelvin body:

$$\varepsilon_{ij}^{ve}=\frac{S_{ij}}{2G_2}\left[1-\exp(-\frac{G_2}{\eta_1\beta}t^{\beta})\right] \tag{27}$$

According to Equation (26) and combined with the three-dimensional form of Newton's viscosity law, the relationship between the viscous deviatoric strain rate and deviatoric stress is as follows:

$$\dot{\varepsilon}_{ij}^{v}=\frac{d\varepsilon_{ij}^{v}}{dt}=\frac{S_{ij}}{2\eta_2} \tag{28}$$

Integrating Equation (28) and rearranging gives the three-dimensional creep equation of the viscous body as:

$$\varepsilon_{ij}^{v}=\int_0^t\frac{S_{ij}}{2\eta_2}dt=\frac{S_{ij}}{2\eta_2}t \tag{29}$$

In the nonlinear rheological model with friction plates, the three-dimensional creep constitutive relation is related to the rock yield function F and plastic potential function Q [33]. Therefore, the three-dimensional creep equation of the nonlinear damage viscoplastic body is:

$$\varepsilon_{ij}^{vp}=\left\{\frac{t_f(1+n)\left[1-(1-D)^n\right]}{2\eta_4 n}+\frac{S_{ij}}{2G_3}\left[1-\exp(-\frac{G_3}{\eta_3\beta}t^{\beta})\right]\right\}\left\langle\Phi(\frac{F}{F_0})\right\rangle\frac{\partial Q}{\partial\sigma_{ij}} \tag{30}$$

Among them,

$$\left\langle\Phi(\frac{F}{F_0})\right\rangle=\begin{cases}0 & (F<0)\\ \Phi(\frac{F}{F_0})=(\frac{F}{F_0})^K & (F\geq 0)\end{cases} \tag{31}$$

where $\left\langle\Phi(\frac{F}{F_0})\right\rangle$ is the switching function. F is the yield function of rock. F_0 is the initial value of the rock yield function, which is generally taken as 1 [34]. K is a specified constant, which is generally taken as 1 [35]. Q is the plastic potential function. Based on the flow rule, $Q=F$ [36].

Therefore, the three-dimensional creep equation of the nonlinear damage viscoplastic body can be simplified as:

$$\varepsilon_{ij}^{vp}=\left\{\frac{t_f(1+n)\left[1-(1-D)^n\right]}{2\eta_4 n}+\frac{S_{ij}}{2G_3}\left[1-\exp\left(-\frac{G_3}{\eta_3\beta}t^{\beta}\right)\right]\right\}\frac{F\partial F}{\partial\sigma_{ij}} \tag{32}$$

For the yield function F in Equation (32), many yield criteria have been proposed to describe it. The Mohr-Coulomb criterion cannot reflect the influence of the intermediate principal stress on the yield behavior of rock. The Mises criterion neglects the effect of spherical stress on the creep behavior of rocks, especially soft rocks. The Drucker-Prager criterion can well remedy the shortcomings of the former two in describing the yield and creep characteristics of rocks. Therefore, the D-P criterion is adopted in this study to characterize the yield function F, whose expression is:

$$F=\sqrt{J_2}-\alpha I_1-k \tag{33}$$

where J_2 is the second invariant of the deviatoric stress tensor. I_1 is the first invariant of the stress tensor. α and k are material parameters.

$$\begin{cases}\alpha=\dfrac{\sin\varphi}{\sqrt{3}\sqrt{3+\sin^2\varphi}}\\ k=\dfrac{\sqrt{3}c\cos\varphi}{\sqrt{3+\sin^2\varphi}}\end{cases} \tag{34}$$

where φ, c are the angle of internal friction and cohesion of the rock, respectively.

In the conventional triaxial graded compression creep test, the following relationship exists:

$$\begin{cases}\sigma_1>\sigma_2=\sigma_3\\ \sigma_m=\dfrac{\sigma_1+\sigma_2+\sigma_3}{3}=\dfrac{\sigma_1+2\sigma_3}{3}\\ \sqrt{J_2}=\dfrac{\sigma_1-\sigma_3}{\sqrt{3}}\\ I_1=\sigma_1+\sigma_2+\sigma_3=\sigma_1+2\sigma_3\\ S_{11}=\sigma_1-\sigma_m=\dfrac{2(\sigma_1-\sigma_3)}{3}\\ \dfrac{\partial F}{\partial\sigma_{11}}=\dfrac{\sqrt{3}-3\alpha}{3}\end{cases} \tag{35}$$

Combining Equations (25), (27), (29), and (32), the creep equation of the three-dimensional nonlinear viscoelastic-plastic damage model can be obtained according to the superposition principle:

(1)When $\dot{\varepsilon}(t \to \infty) = 0, \sigma < \sigma_s$:

$$\varepsilon = \frac{\sigma_1 - \sigma_3}{3G_1} + \frac{\sigma_1 + 2\sigma_3}{9K_1} + \frac{\sigma_1 - \sigma_3}{3G_2}\left[1 - \exp(-\frac{G_2}{\eta_1 \beta} t^{\beta})\right] \tag{36}$$

(2)When $\dot{\varepsilon}(t \to \infty) > 0, \sigma < \sigma_s$:

$$\varepsilon = \frac{\sigma_1 - \sigma_3}{3G_1} + \frac{\sigma_1 + 2\sigma_3}{9K_1} + \frac{\sigma_1 - \sigma_3}{3G_2}\left[1 - \exp(-\frac{G_2}{\eta_1 \beta} t^{\beta})\right] + \frac{\sigma_1 - \sigma_3}{3\eta_2} t \tag{37}$$

(3)When $\sigma > \sigma_s$:

$$\begin{aligned} \varepsilon = & \frac{\sigma_1 - \sigma_3}{3G_1} + \frac{\sigma_1 + 2\sigma_3}{9K_1} + \frac{\sigma_1 - \sigma_3}{3G_2}\left[1 - \exp(-\frac{G_2}{\eta_1 \beta} t^{\beta})\right] + \frac{\sigma_1 - \sigma_3}{3\eta_2} t \\ & + (\frac{1 - \sqrt{3}\alpha}{3})(\sigma_1 - \sigma_3 - \sigma_s)\left\{\frac{t_f(1+n)}{2\eta_4 n}\left[1 - (1-D)^n\right] + \frac{\sigma_1 - \sigma_3}{3G_3}\left[1 - \exp(-\frac{G_3}{\eta_3 \beta} t^{\beta})\right]\right\} \end{aligned} \tag{38}$$

3 Model validation and parameter sensitivity analysis

3.1 Parameter determination and model validation

In the improved model, the parameters to be determined include σ_1, σ_3, σ_s, G_1, K_1, G_2, η_1, η_2, t_f, G_3, η_3, η_4, n, α, β, with a total of 15 parameters. Parameters such as σ_1, σ_3, σ_s, E, μ, and φ can be obtained through uniaxial compression and triaxial compression experiments. The shear modulus $G_1=E/2(1+\mu)$, and the bulk modulus $K_1=E/3(1-2\mu)$. According to the value of the rock internal friction angle φ, the parameter α can be calculated in combination with Equation (34). Based on the results of compressive creep tests, the slope ψ of the curve in the steady creep stage is calculated. From $\psi=(\sigma_1-\sigma_3)/3\eta_2$, we can obtain $\eta_2=(\sigma_1-\sigma_3)/3\psi$. Meanwhile, the time t_f for creep failure of the rock can be obtained. According to Equation (8), the damage variable$D$ can be obtained when t_f and n are known. The remaining seven parameters G_2, G_3, η_1, η_3, η_4, β, and n need to be identified through model parameter identification.

The 1stOpt software adopts a universal global optimization algorithm, which can obtain all optimal solutions from arbitrary random initial values [37]. In this study, the differential evolution-universal global optimization (DE-UGO) algorithm is adopted based on the 1stOpt software to invert the above seven parameters. This algorithm generates an initial population randomly, and conducts iterative optimization through mutation, crossover and selection operations, overcoming the sensitivity of traditional local optimization algorithms to initial values.

The objective function for parameter identification is defined as the root-mean-square error between the calculated values of the model and the experimental measured values:

$$RMSE = \sqrt{\frac{1}{n}\sum\nolimits_{i=1}^{n}(Y_i^{test} - Y_i^{cal})^2} \tag{39}$$

where *RMSE* denotes the root-mean-square error. The subscripts Y_i^{test} and Y_i^{cal} represent the experimental measured values and the model calculated values, respectively.

The convergence criteria are set as follows: (1) The maximum number of evolutionary generations is 1000. (2) RMSE<1×10^{-8}. (3) The variation amplitude of the objective function value is less than 1×10^{-10} in 50 consecutive iterations. The calculation terminates when any of the conditions is satisfied.

To quantitatively evaluate the accuracy of the parameter inversion results, the coefficient of determination is introduced:

$$R^2 = 1 - \frac{\sum\nolimits_{i=1}^{n}(Y_i^{test} - Y_i^{cal})^2}{\sum\nolimits_{i=1}^{n}(Y_i^{test} - \bar{Y}^{test})^2} \tag{40}$$

where R^2 is the coefficient of determination, and $\bar{Y}^{test}$ is the average value of experimental measured data.

During the parameter identification process, when the stress level applied in the creep test is lower than the yield strength of the rock, Equation (25) is used to fit the rock creep curve. When the stress level is higher than the yield strength, Equation (26) is used to fit the rock creep curve. First, Equation (25) is used to fit the transient creep stage and the steady creep stage, so as to determine the values of parameters G_2, η_1, and β. Then, keeping these parameters unchanged, Equation (26) is used to fit the full creep curve and determine the values of parameters G_3, η_3, η_4, and n.

Liu Dongyan et al. [38] conducted uniaxial and triaxial compression experiments on sandstone using an MTS815 system. The basic mechanical parameters are listed in Table 1. Uniaxial and triaxial compression creep tests on sandstone were carried out using an RLW-2000 testing system. The confining pressures were set to 0 MPa, 5 MPa, 10 MPa, and 15 MPa, respectively. An axial force-controlled loading scheme was adopted with a loading rate of 1 kN/s. The experiments were conducted at room temperature.

Table 1 Experimental results of sandstone compression mechanical properties [38]

Confining pressure/MPa	$(\sigma_1-\sigma_3)_{max}$/MPa	$(\sigma_1-\sigma_3)_s$/MPa	E/GPa
0	50.09	38.82	6.97
5	65.10	51.11	12.40
10	80.12	60.59	15.67
15	93.92	71.75	17.53

Combined with the experimental results of Liu Dongyan et al. [38], the model parameters identified using the 1stOpt software are listed in Tables 2 and 3. It can be seen from Tables 2 and 3 that the coefficients of determination R^2 of the identification results all exceed 0.95, indicating favorable accuracy. After all model parameters were determined, the fitting curves were generated using the 1stOpt software. A comparison between the fitting curves and the experimental curves is shown in Figure 3. It can be seen that the improved model can well predict the creep evolution characteristics of sandstone.

Table 2 Identification results of uniaxial compression creep model parameters

Stress /MPa	E_1/MPa	E_2/MPa	E_3/MPa	η_1/MPa • h	η_2/MPa • h	η_4/MPa • h	n	η_3/MPa •h	β	R^2
48.92	7498	19521	2946	0.2	0.002	2.489	10.646	556	0.728	0.997

Table 3 Identification results of triaxial compression creep model parameters

Pressurization/ MPa	Stress /MPa	G_1/MPa	K_1/MPa	G_2/MPa	η_1/MPa • h	η_2/MPa • h	η_4/MPa • h	n	G_3/MPa	η_3/MPa • h	β	R^2
5	63.80	13962	1589	38527	0.045	54929	1339	4.95	98465	39959	0.7	0.999

10	78.52	14023	3733	8.55	10.98	14898	14632	0.009	1.71	9.79	8.47	0.999
15	84.52	21244	4525	22843	39548	93018	46633	0.0008	335332	22676	20.59	0.994

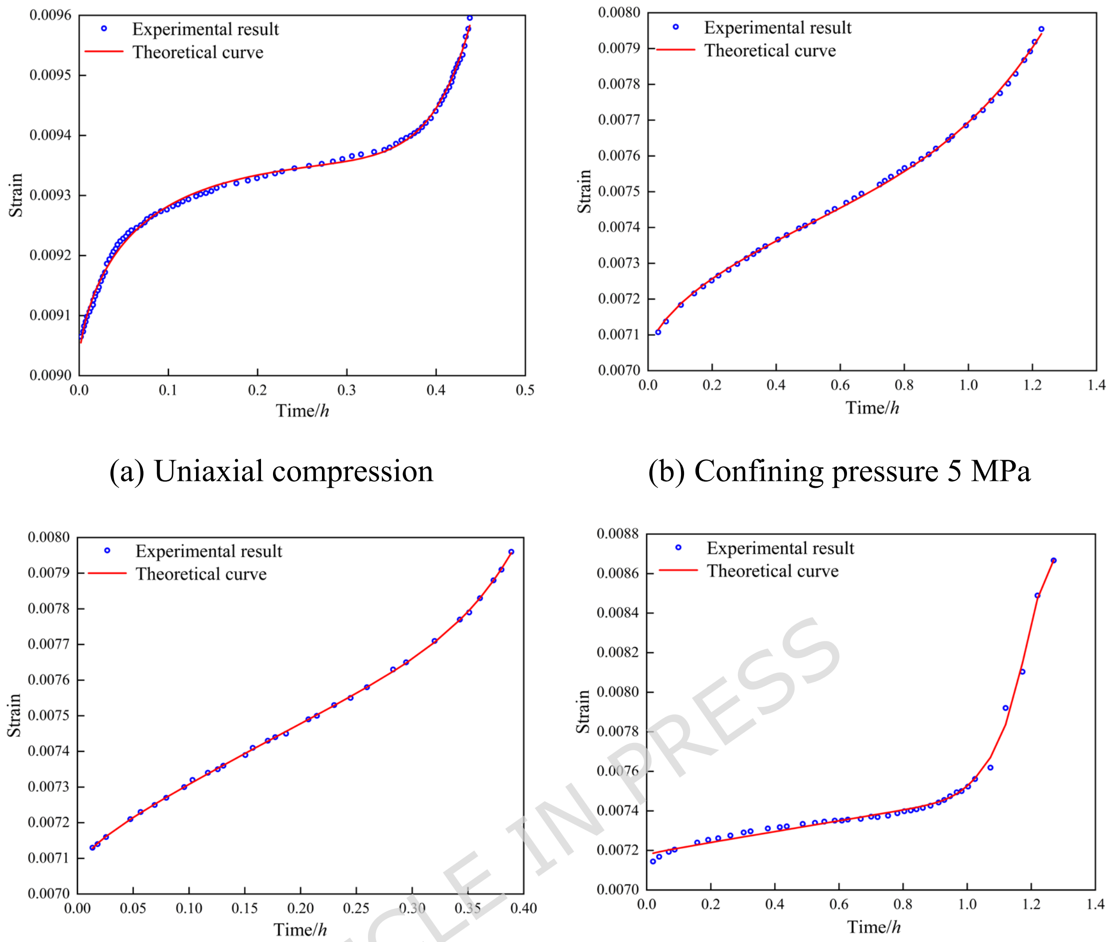

(a) Uniaxial compression (b) Confining pressure 5 MPa

(c) Confining pressure 10 MPa (d) Confining pressure 15 MPa

Fig. 3 Comparison of creep test curve with theoretical curve

3.2 Parameter sensitivity analysis

Since the improved model involves many parameters, sensitivity analysis of the model parameters is very important. In this study, the strain rate is taken as the sensitivity evaluation index to carry out parameter sensitivity analysis.

$$\delta\varepsilon = \frac{\varepsilon^{'} - \varepsilon}{\varepsilon} \tag{41}$$

where $\delta\varepsilon$ is the strain rate, and $\varepsilon^{'}$ and ε represent the strains before and after parameter variation, respectively.

Based on the model data in Tables 2 and 3, any single parameter is adjusted to -40%, -20%, 20%, and 40% of its baseline value. Only one parameter is adjusted each time, while the others remain unchanged. The strain rate is calculated, and the parameter sensitivity analysis diagram is plotted, as shown in Figure 4. A parameter is considered to which the rock creep strain is sensitive when the absolute value of the strain change rate exceeds 10% [39].

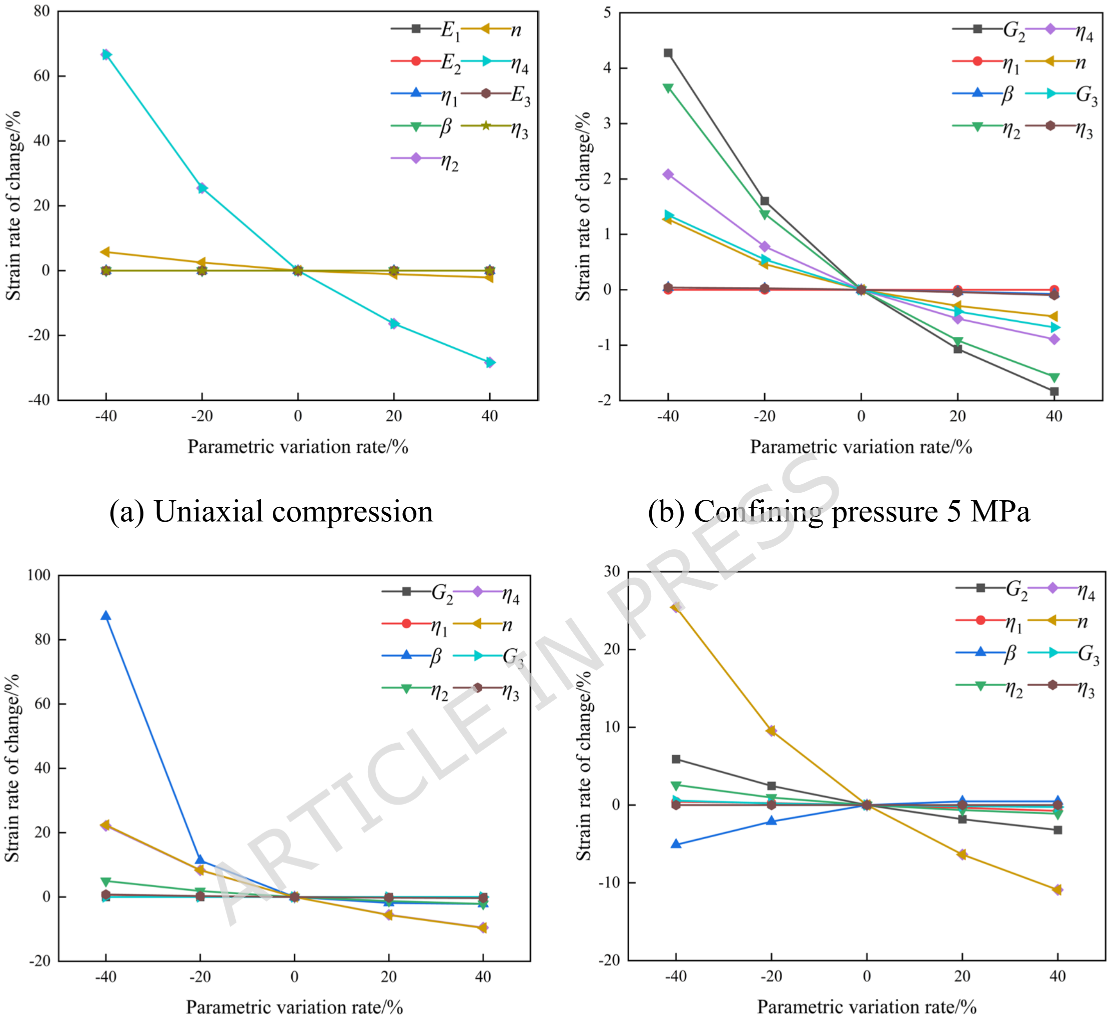

(a) Uniaxial compression

(b) Confining pressure 5 MPa

(c) Confining pressure 10 MPa

(d) Confining pressure 15 MPa

Fig. 4 Sensitivity analysis of model parameters

It can be seen from Figure 4(a) that in the uniaxial compression creep test, the strain is most sensitive to changes in parameters η_2 and η_4. The fundamental reason is that these two parameters dominate the time-dependent deformation mechanism. η_2 directly determines the development rate of viscoelastic strain in the decelerating creep stage by controlling the relaxation time of the nonlinear Kelvin body. It governs how rapidly the strain approaches its asymptotic value from the instantaneous value, thus exerting a decisive influence on the strain magnitude during the early and middle stages of creep. η_4 directly determines the linear accumulation rate of viscoplastic strain over time. This irrecoverable deformation constitutes the primary source of the total strain increment during long-term creep.

It can be seen from Figure 4(b) that in the triaxial compression creep test under low confining pressure, the sensitivity of strain to changes in all parameters is less than 5%. At a low confining pressure of 5 MPa, the rock remains in a brittle state. The total strain is dominated by instantaneous elastic strain, and the time-dependent creep deformation is not significant. Therefore, the strain exhibits extremely low sensitivity to both the elastic parameters governing the instantaneous response and the viscous parameters controlling the time-dependent effect.

It can be seen from Figure 4(c) that at a confining pressure of 10 MPa, the strain is most sensitive to changes in parameters β and n. This is because when the confining pressure increases to 10 MPa, the rock transforms from brittle to ductile, and the decelerating creep stage develops fully. At this point, the exponent β, which governs nonlinear decelerating creep, becomes a key parameter determining the initial strain accumulation rate. Meanwhile, the damage variable D begins to evolve, and the damage index n significantly affects the creep life and strain development by controlling the damage accumulation rate (Equation (7)). Together, the two parameters dominate the strain response under this confining pressure.

It can be seen from Figure 4(d) that at a confining pressure of 15 MPa, the strain is most sensitive to changes in parameters n and η_4. This is because as the confining pressure further increases, the rock enters a highly ductile or semi-plastic state. High confining pressure compresses the time window of the decelerating creep stage, resulting in a decrease in the sensitivity of β. Deformation becomes dominated by accelerated creep. η_4 controls the strain rate in the accelerated creep stage, while n determines the evolution curvature of accelerated creep by governing the damage accumulation rate.

The sensitivity of strain to model parameters varies with different confining pressure conditions. The fundamental reason is that confining pressure alters the macroscopic deformation mechanism of rock, thereby activating different controlling parameters.

4 Conclusion

(1) Based on modifications to the nonlinear Kelvin body and the nonlinear damage viscoplastic body, this study proposes an improved nonlinear viscoelastic-plastic damage model for rock. The constitutive equations of the improved model are derived, and the expressions for one-dimensional and three-dimensional creep equations are presented.

(2) Based on the mechanical test results, the determination methods for model parameters including σ_1, σ_3, σ_s, G_1, K_1, η_2, t_f, and α are presented. Based on the universal global optimization algorithm in the 1stOpt software, an inversion method is proposed for the seven parameters includingG_2, G_3, η_1, η_3, η_4, β, and n. The coefficient of determination R^2 of the identification results all exceeds 0.95, indicating favorable accuracy. The fitting curves of the improved model are in good agreement with the experimental curves, which can well predict the creep evolution characteristics of sandstone.

(3) Using the strain change rate as the sensitivity evaluation index, a systematic analysis was conducted on the sensitivity of the improved model parameters. In uniaxial compression creep tests, strain is most sensitive to η_2 and η_4. At a confining pressure of 5 MPa, the sensitivity of strain to all parameters is less than 5%. When the confining pressure is increased to 10 MPa, the strain shows the highest sensitivity to β and n. When the confining pressure is further increased to 15 MPa, the strain is most sensitive to n and η_4. These results reflect the fundamental transition of rock creep mechanisms with increasing confining pressure.

(4) The improved model still has certain limitations, which need to be further investigated in future research. For example, the present model does not yet consider the influences of lithology, stress path, temperature, and other factors. The general applicability of the damage evolution function needs to be systematically investigated.

Acknowledgments

This study was supported by the Guizhou Science and Technology Support

Program Project (Qian Ke He Zhi Cheng [2026] General No. 305), Guizhou Science and Technology Plan Project (Qian Ke He Ji Chu QN [2025] No. 223), Scientific Research Startup Project for High-Level Talents, Guizhou Institute of Technology (2025GCC023), and Science and Technology Program of Guizhou Province (Qiankehe Platform KXJZ [2024]020). All of the support provided is gratefully acknowledged.

Author contributions

Xingchao TIAN: Validation, Data curation, Writing - original draft. Benchao JIA, Dingyu SUN and Zhen CHENG: Organizing and analyzing experimental data. Tiejun TAO: Methodology, Writing - review & editing.

Funding

The Guizhou Science and Technology Support Program Project (Qian Ke He Zhi Cheng [2026] General No. 305), Guizhou Science and Technology Plan Project (Qian Ke He Ji Chu QN [2025] No. 223), Scientific Research Startup Project for High-Level Talents, Guizhou Institute of Technology (2025GCC023), and Science and Technology Program of Guizhou Province (Qiankehe Platform KXJZ [2024]020).

Declaration of competing interest

The authors declare no competing interests.

Data Availability

The datasets used during the current study available from the corresponding author on reasonable request.

References

[1] Zhou X.P., Pan X.K., Berto F. A state-of-the-art review on creep damage mechanics of rocks [J]. Fatigue and Fracture of Engineering Materials and Structures. 2022, 45(3): 627-652. DOI: 10.1111/ffe.13625.

[2] Tarifard A., Török A., Görög P.. Review of the creep constitutive models for rocks and the application of creep analysis in geomechanics [J]. Rock Mechanics and Rock Engineering, 2024, 57: 7727-7757. DOI: 10.1007/s00603-024-03939-x.

[3] Yang J.N., Fan P.X., Wang M.Y., et al. Perturbation-induced delayed shear creep instability in rock joints: A nonlinear model based on irreversible deformation [J]. International Journal of Rock Mechanics and Mining Sciences, 2025, 195: 106289. DOI: 10.1016/j.ijrmms.2025.106289.

[4] Yang J, Fan P, Wang J, et al. Energy characteristics during the progressive shear failure of rock joints and brittleness evaluation [J]. International Journal of Mining Science and Technology, 2026, 36(4). DOI: https://doi.org/10.1016/j.ijmst.2026.03.004.

[5] Fang C.F., Mei G.X., Yu W.J., et al. The effect of roundness on single particle crushing under multi-contact loading via the DEM [J]. Computers and Geotechnics, 2026, 195.

[6] Fang C.F., Zhao T.Y., Yu W.J., et al. Effect of pore shape on uniaxial compressive behaviour of porous rock-like materials: DEM simulation [J]. Case Studies in Construction Materials, 2025: e04938. DOI: 10.1016/j.cscm.2025.e04938.

[7] Fang C.F., Mei G.X.,Yu W.J., et al. DEM for investigating the mechanical properties of porous rock-like materials under uniaxial compression [J]. Computers and Geotechnics, 2024, 170: 106307. DOI: 10.1016/j.compgeo.2024.106307.

[8] Liu Y.Q , He C., Yao C.F., et al. Responses of a tunnel crossing a strike-slip fault considering the interaction of fault creep and creep of surrounding rock [J]. Tunnelling and Underground Space Technology, 2025, 164: 106827. DOI: 10.1016/j.tust.2025.106827.

[9] Yang J.T., Song Y.Q., Hao Z.B., et al. A Fractional Full-Stage Creep Prediction Model for Salt Rock Based on Stress Threshold and Damage Evolution [J]. Rock Mechanics and Rock Engineering, 2025, 58(12): 13089-13111. DOI: 10.1007/s00603-025-04815-y.

[10] Chen D.X., Wang L.G., Wang S.Y., et al. Macroscopic Creep Damage Fracture Characteristics and Microscopic Mechanisms of Microporous Defective Sandstone [J]. Rock Mechanics and Rock Engineering, 2025, 58(9): 10695-10715. DOI: 10.1007/s00603-025-04669-4.

[11] Liu R., Zhou S.W., Qin S.K., et al. A phase field fracture model for rock creep: Theoretical framework and engineering applications [J]. Computers and Geotechnics, 2026, 193: 108007. DOI: 10.1016/j.compgeo.2026.108007.

[12] Chen Y., Chen Q., Pan Y., et al. A Chemical Damage Creep Model of Rock Considering the Influence of Triaxial Stress. Materials, 2022, 15: 7590. DOI: https://doi.org/10.3390/ma15217590.

[13] Zhang L.L., Wang X.J.. Rock damage creep model based on generalized Burgers model [J]. Chinese Journal of Safety Science, 2019, 29(01): 125-131. DOI: 10.16265/j.cnki.issn1003-3033.2019.01.02.

[14] Zhao Y., Wang Y., Wang W., et al. Modeling of non-linear rheological behavior of hard rock using triaxial rheological experiment [J]. International Journal of Rock Mechanics and Mining Sciences, 2017, 93: 66-75. DOI: 10.1016/j.ijrmms.2017.01.004.

[15] Zhao B., Wang B., Huang W., et al. The nonlinear creep behavior and creep damage constitutive model of coal rock [J]. Arabian Journal of Geosciences, 2023(3): 16. DOI: https://doi.org/10.1007/s12517-023-11280-w.

[16] Wei E.J., Hu B., Li J., et al. Nonlinear Viscoelastic-Plastic Creep Model of Rock Based on Fractional Calculus [J]. Advances in Civil Engineering, 2022, 2022(Pt.1): 1.1-1.7. DOI: https://doi.org/10.1155/2022/3063972.

[17] Bu P., Li Y.L., Li Y., et al. Creep damage coupling model of concrete based on the statistical damage theory [J]. Journal of Building Engineering, 2022. DOI: https://doi.org/10.1016/j.jobe.2022.105437.

[18] Liu H.Z., Xie H.Q., He J.D., et al. Nonlinear creep damage constitutive model for soft rocks [J]. Mechanics of Time Dependent Materials, 2017. DOI: 10.1007/s11043-016-9319-7.

[19] Meng L., Chen W.F., Yan Y.B., et al. Modelling of creep and plasticity deformation considering creep damage and kinematic hardening [J]. Engineering Fracture Mechanics, 2019, 218. DOI: https://doi.org/10.1016/j.engfracmech.2019.106582.

[20] Yu C., Tang S., Tang C., et al. The effect of water on the creep behavior of red

sandstone [J]. Engineering Geology, 2019, 253: 64-74. DOI: 10.1016/j.enggeo.2019.03.016.

[21] Zhu W.C., Li S.H., Li S., et al. Influence of Dynamic Disturbance on the Creep of Sandstone: An Experimental Study [J]. Rock Mechanics and Rock Engineering, 2019, 52(4). DOI: 10.1007/s00603-018-1642-7.

[22] Chu Z., Wu Z., Wang Z., et al. Micro-mechanism of brittle creep in saturated sandstone and its mechanical behavior after creep damage [J]. International Journal of Rock Mechanics and Mining Sciences, 2022(149): 149. DOI: 10.1016/j.ijrmms.2021.104994.

[23] Xu T., Zhou G.L., Heap M.J., et al. The Modeling of Time-Dependent Deformation and Fracturing of Brittle Rocks Under Varying Confining and Pore Pressures [J]. Rock Mechanics and Rock Engineering, 2018. DOI: 10.1007/s00603-018-1491-4.

[24] Wang R., Zhuo Z., Zhou H.W., et al. A fractal derivative constitutive model for three stages in granite creep [J]. Results in Physics, 2017: S2211379717310239. DOI: 10.1016/j.rinp.2017.07.051.

[25] Xu W.Y., Yang S.Q., Xie S.Y., et al. Study on triaxial rheological mechanical properties of greenschist (II): Model analysis [J]. Geomechanics, 2005(05): 693-698. DOI: 10.16285/j.rsm.2005.05.004.

[26] Zhao B.Y., Liu D.Y., Zheng Z.N., et al. Study on nonlinear viscoelastic-plastic creep model of rock based on short-term triaxial creep test [J]. Journal of Mining and Safety Engineering, 2011, 28(03): 446-451.

[27] Li Y.L., Yu H.C., Liu H.D.. Creep constitutive model of silty mudstone under triaxial compression [J]. Geomechanics, 2012,33(07): 2035-2040+2047. DOI: 10.16285/j.rsm.2012.07.009.

[28] Zhang Z.L., Xu W.Y., Wang W.. Triaxial creep test and nonlinear viscoelastic-plastic creep model of rock in the compression zone of dam foundation of Xiangjiaba Hydropower Station [J]. Rock Mechanics and Engineering, 2011, 30(01): 132-140.

[29] Cao P., Wen Y.D., Wang Y.X., et al. Study on nonlinear damage creep constitutive

model for high-stress soft rock [J]. Environmental Earth Sciences, 2016, 75(10): 900-908. DOI: 10.1007/s12665-016-5699-x.

[30] KACHANOV M.. Effective elastic properties of cracked solids: critical review of some basic concepts [J]. Mechanics Reviews, 1992, 45(8): 304-335. DOI: 10.1115/1.3119761.

[31] Zhang L.L., Wang X.J.. Study on viscoelastic-plastic damage creep model of rock [J]. Journal of Geotechnical Engineering, 2020, 42(06): 1085-1092.

[32] Wang J.B., Liu X.R., Song Z.P., et al. An improved Maxwell creep model for salt rock [J]. Geotechnical Mechanics and Engineering, 2015, 9(4): 499-511. DOI: 10.12989/gae.2015.9.4.499.

[33] Qi Y.J., Jiang Q.H., Wang Z.J., et al. Improved three-dimensional creep constitutive equation of Nishihara model and its parameter identification [J]. Journal of Rock Mechanics and Engineering, 2012, 31(02): 347-355.

[34] Perzyna P.. Fundamental Problems in Viscoplasticity [J]. Advances in Applied Mechanics, 1966, 10(2):2 43. DOI: 10.1016/S0065-2156(08)70009-7.

[35] Al-Rub R.K.A., Darabi M.K., Kim S.M., et al. Mechanistic-based constitutive modeling of oxidative aging in aging-susceptible materials and its effect on the damage potential of asphalt concrete [J]. Construction and Building Materials, 2013, 41(apr.): 439-454. DOI: 10.1016/j.conbuildmat.2012.12.044.

[36] Moghadam S.N., Mirzabozorg H., Noorzad A.. Modeling time-dependent behavior of gas caverns in rock salt considering creep, dilatancy and failure [J]. Tunnelling and Underground Space Technology, 2013, 33: 171-185. DOI: 10.1016/j.tust.2012.10.001.

[37] Cheng X.Y., Zhang W., Hu S.Y., et al. Optimization Fitting Modeling: 1stOpt Application Description [M]. China Building Materials Industry Press, 2012.

[38] Liu D.Y., Xie L.J., Tuo X.F., et al. Creep characteristics and nonlinear viscoelastoplastic model of sandstone under different confining pressures [J]. Journal of Rock Mechanics and Engineering, 2017, 36(A02): 8. DOI: CNKI: SUN: YSLX.0.2017-S2-001.

[39] Wang Z.L., Bi C.V., Li H.R.. Numerical simulation of concrete blasting damage

by SPH-FEM coupling method [J]. Explosion and impact, 2018, 38(06): 1419-1428.